Inorg. Chem. **2005**, *44*, 2973–2982

Formation of N–I Charge-Transfer Bonds and Ion Pairs in Polyiodides with Imidotellurium Cations

Jari Konu,[†] Tristram Chivers,*[,‡] Gabriele Schatte,[‡] Masood Parvez,[‡] and Risto S. Laitinen*[,†]

Department of Chemistry, University of Oulu, P.O. Box 3000, 90014 Oulu, Finland, and University of Calgary, 2500 University Drive N.W., Calgary, Alberta, Canada T2N 1N4

Received January 14, 2005

[(^{t}BuNH)Te(μ-N^{t}Bu)$_2$Te(N^{t}Bu)][OSO$_2$CF$_3$] (**4a**) is obtained in quantitative yields by the treatment of [(^{t}BuN)-Te(μ-N^{t}Bu)$_2$Te(N^{t}Bu)] (**1**) with HCF$_3$SO$_3$. The reaction of **4a** with LiI and iodine in the molar ratio 1:1:4.5 affords a product that, upon recrystallization from acetonitrile, was found to be a solid solution of [(^{t}BuNH)Te(μ-N^{t}Bu)$_2$-Te(N^{t}Bu)]$_2$I$_{20}$ (**5a**) and [(^{t}BuNH)Te(μ-N^{t}Bu)$_2$Te(NH^{t}Bu)]$_2$I$_{18}$ (**5b**). Consequently, the crystal structure is disordered, containing 88.3(1)% of **5a**·2MeCN and 11.7(1)% of **5b**·2MeCN. The I$_{20}$ framework is involved in two symmetry-equivalent N–I–I–I–I fragments, two I$_3^-$ ions, and three I$_2$ molecules that are linked together by I···I secondary bonding interactions. The bonding in the N–I–I–I–I fragment can be considered in terms of the lp(N) → σ^*(I$_2$) and π^*(I$_2$) → σ^*(I$_2$) charge-transfer interactions involving one [(^{t}BuNH)Te(μ-N^{t}Bu)$_2$Te(N^{t}Bu)]$^+$ cation and two I$_2$ units. The N–I bond length of 2.131(7) Å, the I–I distances of 3.118(1), 3.095(2), and 2.788(2) Å, and the ∠I$_2$ –I$_2$ angle of 84.75(4)° are consistent with this bonding scheme. The I–I bond distances in the two symmetry-equivalent I$_3^-$ ions are 3.113(1) and 2.792(2) Å, and those in two crystallographically independent I$_2$ molecules are 2.736(2) and 2.743(1) Å. The formal I$_{18}^{4-}$ anion in **5b**·2MeCN consists of four I$_3^-$ anions and three I$_2$ molecules linked by I···I secondary bonds. One crystallographically independent I$_3^-$ anion is connected to the [(^{t}BuNH)Te(μ-N^{t}Bu)$_2$-Te(HN^{t}Bu)]$^{2+}$ cation by two hydrogen bonds [H···I = 2.823(5) and 2.983(5) Å; N···I = 3.697(8) and 3.857(9) Å]. The I$_3^-$ anions and I$_2$ molecules in **5b** show virtually identical bond parameters to those in **5a**. The treatment of **1** with iodine and the reactions of its methylated derivatives, [(^{t}BuNMe)Te(μ-N^{t}Bu)$_2$Te(N^{t}Bu)][OSO$_2$CF$_3$] and [(^{t}BuNMe)-Te(μ-N^{t}Bu)$_2$Te(MeN^{t}Bu)][OSO$_2$CF$_3$]$_2$, with LiI and iodine also afford highly moisture-sensitive polyiodides, either by the formation of N–I charge-transfer complexes or by ionic interactions. The crystal structures of the partially hydrolyzed products, [(^{t}BuIN)Te(μ-N^{t}Bu)$_2$Te(μ-O)]$_2$(I$_3$)$_2$ (**3**), [(^{t}BuMeN)Te(μ-N^{t}Bu)$_2$Te(μ-O)]$_2$(I$_3$)$_2$ (**6**), and **6**·2MeCN, are also reported.

Introduction

Tellurium diimides exhibit different structures and reactivities compared to those of their sulfur or selenium analogues. For example, the tellurium diimides, [(RN)Te-(μ-NR′$_2$Te(NR)] (R = R′ = ^{t}Bu; R = PPh$_2$NSiMe$_3$, R′ = ^{t}Bu, ^{t}Oct),[1–3] are dimeric, whereas the sulfur diimides are invariably monomers.[4–8] Only two selenium diimides, (RN)$_2$Se (R = 1-adamantyl, C$_6$H$_2$^{t}Bu$_3$),[9,10] have been structurally characterized, and both are monomeric. The tellurium diimide [(^{t}BuN)Te(μ-N^{t}Bu)$_2$Te(N^{t}Bu)] (**1**) is readily prepared in high yields and isolated as the *cis-endo,endo* isomer. This reagent is a source of other thermally stable tellurium−nitrogen

* Authors to whom correspondence should be addressed. E-mail: chivers@ucalgary.ca. Tel: (403) 220-5741. Fax: (403) 289-9488 (T.C.). E-mail: risto.laitinen@oulu.fi. Tel: (3588) 553-1611. Fax: (3588) 553-1608 (R.S.L.).
[†] University of Oulu.
[‡] University of Calgary.

(1) Chivers, T.; Gao, X.; Parvez, M. *J. Chem. Soc., Chem. Commun.* **1994**, 2149.
(2) Chivers, T.; Gao, X.; Parvez, M. *J. Am. Chem. Soc.* **1995**, *117*, 2359.
(3) Chivers, T.; Gao, X.; Parvez, M. *Inorg. Chem.* **1996**, *35*, 9.
(4) Suenram, R. D.; Lovas, F. J.; Stevens, W. J. *J. Mol. Spectrosc.* **1985**, *112*, 482.
(5) Kuyper, J.; Isselmann, P. H.; Mijlhoff, F. C.; Spelbos, A.; Renes, G. *J. Mol. Struct.* **1975**, *29*, 247.
(6) Herberhold, M.; Gerstmann, S.; Milius, W.; Wrackmeyer, B.; Bormann, H. *Phosphorus, Sulfur Silicon Relat. Elem.* **1996**, *112*, 261.
(7) Herberhold, M.; Gerstmann, S.; Milius, W.; Wrackmeyer, B.; Bormann, H. *J. Chem. Soc., Dalton Trans.* **1994**, 633.
(8) Bagryanskaya, I. Y.; Gatilov, Y.; Shakirov, M. M.; Zibarev, A. V. *Mendeleev Commun.* **1994**, 136.
(9) Maaninen, T.; Laitinen, R.; Chivers, T. *Chem. Commun.* **2002**, 1812.

10.1021/ic050058k CCC: $30.25
Published on Web 03/22/2005

compounds. For example, reactions of **1** with KO^{t}Bu or ^{t}BuNHLi afford the pyramidal anions $[Te(N^tBu)_2(O^tBu)]^-$ and $[Te(N^tBu)_3]^{2-}$, respectively.[11−13] The cycloaddition reaction of **1** with ^{t}BuNCO produces the dimeric ureatotelluroxide $[OC(\mu\text{-}N^tBu)_2TeO]_2$, which forms an extended helical network in the solid state as a result of weak C═O···Te interactions.[14] The chelation of dimer **1** to the Ag(I) center results in the *cis-exo,exo* arrangement of the exocyclic N^{t}Bu groups.[15,16] By contrast, the coordination of **1** to Cu(I) affords a dinuclear complex, in which the dimer acts either as a terminal monodentate or as a bridging bidentate ligand. In the bridging ligand, the exocyclic N^{t}Bu groups are in a *trans-exo,exo* arrangement, whereas they occupy *cis-endo,exo* positions in the terminal ligands.[15,16]

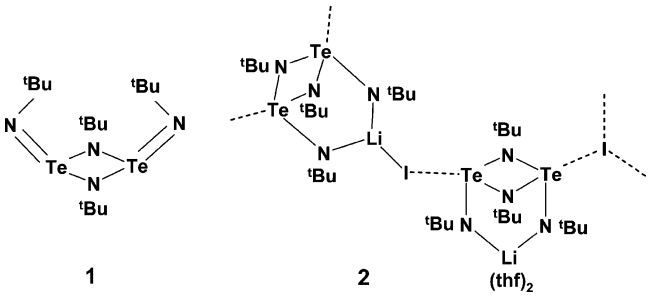

Recently, we reported that the reaction of **1** with LiI produces $\{Li(THF)_2[Te_2(N^tBu)_4]\}(\mu_3\text{−}I)\{LiI[Te_2(N^tBu)_4]\}$ (**2**; THF = tetrahydrofuran), a complex exhibiting two different types of Te···I interactions.[17] Complex **2** is also formed in the oxidation of $[Te(N^tBu)_3]^{2-}$ with iodine.[17] The initial objective of the current work was to determine the outcome of the oxidation of **1** by iodine. Investigations of this reaction at different stoichiometries revealed the formation of products containing an N−I bond and polyiodide counterions. Polyiodides have attracted interest in view of their versatile structural features and high electrical conductivities.[18] Ions with compositions ranging from I_3^- to I_{29}^{3-} have been structurally characterized.[18] Consequently, this investigation was broadened to include a survey of the use of protonated or methylated derivatives of **1** as templates in the formation of polyiodides. We report here that the reaction of the monoprotonated derivative $[(^t\text{BuNH})Te(\mu\text{-}N^tBu)_2Te(N^tBu)][OSO_2CF_3]$ (**4a**) with a mixture of LiI and iodine affords a product that, upon recrystallization from acetonitrile, was found to contain $[(^t\text{BuNH})Te(\mu\text{-}N^tBu)_2Te(N^tBu)]_2I_{20}$ (**5a**) and $[(^t\text{BuNH})Te(\mu\text{-}N^tBu)_2Te(NH^tBu)]_2I_{18}$ (**5b**). The crystal structures of $[(^t\text{BuIN})Te(\mu\text{-}N^tBu)_2Te(\mu\text{-}O)]_2(I_3)_2$ (**3**), **4a**, **5**·2MeCN, $[(^t\text{BuMeN})Te(\mu\text{-}N^tBu)_2Te(\mu\text{-}O)]_2(I_3)_2$ (**6**), and its acetonitrile solvate **6**·2MeCN are also reported.

Experimental Section

General Procedures. All reactions and manipulations of air- and moisture-sensitive reagents were carried out under dry argon. The reagents $TeCl_4$ (Acros), *n*-butyllithium (2.5 M in hexanes), ^{t}BuNH$_2$, HCF_3SO_3, $MeCF_3SO_3$, LiI, and I_2 (Aldrich) were used without further purification. **1**,[19,20] $[(^t\text{BuNMe})Te(\mu\text{-}N^tBu)_2TeN^tBu][OSO_2CF_3]$, and $[(^t\text{BuNMe})Te(\mu\text{-}N^tBu)_2Te(MeN^tBu)][OSO_2CF_3]_2$ were prepared by the procedures described earlier.[16] Hexane, toluene, and THF were dried by distillation over Na/benzophenone; CH_2Cl_2 was dried over P_4O_{10}; and acetonitrile was dried over CaH_2 (or P_4O_{10}) under a nitrogen atmosphere immediately prior to use.

Spectroscopic Methods. The ^{1}H NMR spectra were recorded in d_8-toluene, CD_2Cl_2, and CD_3CN on a Bruker DPX 200 spectrometer operating at 200.131 MHz. The spectral width was 41.25 kHz, yielding a resolution of 0.42 Hz/data point. The ^{7}Li, ^{13}C, and ^{125}Te NMR spectra were recorded in THF, toluene, CH_2Cl_2, and MeCN on a Bruker DPX 400 spectrometer operating at 155.505, 100.623, and 126.240 MHz, respectively. The spectral widths were 70.02, 30.30, and 95.24 kHz, respectively, yielding respective resolutions of 0.43, 0.62, and 1.45 Hz/data point. The ^{7}Li, ^{13}C, and ^{125}Te NMR spectra were recorded unlocked. The ^{1}H and ^{13}C variable-temperature NMR spectra were measured in deuterated toluene on a Bruker AM 400 spectrometer operating at 399.873 and 100.559 MHz. The spectral widths in these measurements were 47.89 and 25.13 kHz, respectively, yielding respective resolutions of 0.29 and 0.77 Hz/data point. ^{1}H and ^{13}C NMR spectra are referenced to the solvent signal and are reported relative to Me_4Si. The ^{125}Te NMR spectra are referenced externally to a saturated solution of H_6TeO_6, and the ^{125}Te chemical shifts are reported relative to Me_2Te [$\delta(Me_2Te) = \delta(H_6TeO_6) + 712$].

Raman spectra were recorded from solid samples at room temperature by using a Bruker IFS-66 spectrometer equipped with a FRA-16 Raman unit and a Nd:YAG laser (power, 110 mW; scans, 8−64; spectral resolution, ±1 cm^{-1}; Blackmann−Harris four-term apodization, no white light correction; scattering geometry, 180°). The IR spectra of **4a** and **5** were measured as Nujol mulls between KBr plates on a Mattson Genesis Series Fourier transform infrared- (4000−300 cm^{-1}) spectrometer. Elemental analyses were performed by Analytical Services, Department of Chemistry, University of Calgary.

Reactions of 1 with I_2. A series of reactions was carried out in which a solution of **1** (0.270 g, 0.50 mmol) in toluene (20 mL) was added to a solution of I_2 (0.50, 1.50, 2.50, and 5.00 mmol) in toluene (20 mL) cooled to −80 °C. Each reaction mixture was stirred for 1 h at −80 °C and for 3−20 h at 23 °C. The solvent was evaporated under a vacuum to give a red powder. The intensity of the red color was dependent on the amount of iodine used. Yields of the products were ca. 90%, except in the case of the 1:10 molar ratio, for which the yield was ca. 55%. ^{1}H NMR (CD_3CN): (molar ratio 1:1) δ 1.58 (18H), 1.47 (18H); (molar ratio 1:3) δ 1.57 (18H), 1.48 (br); (molar ratio 1:5) δ 1.58 (18H), 1.57 (9H), 1.47 (9H); (molar ratio 1:10) δ 1.58 (27H, br, sh), 1.47 (9H). Red crystals of **3** were obtained from CH_3CN solutions at −20 °C in the reactions in which the molar ratio of **1** and I_2 were 1:3 or 1:5.

(10) Maaninen, T.; Tuononen, H. M.; Kosunen, K.; Oilunkaniemi, R.; Hiitola, J.; Laitinen, R.; Chivers, T. *Z. Anorg. Allg. Chem.* **2004**, 630, 1947.
(11) Chivers, T.; Gao, X.; Parvez, M. *Inorg. Chem.* **1996**, *35*, 553.
(12) Chivers, T.; Gao, X.; Parvez, M. *Angew. Chem., Int. Ed. Engl.* **1995**, *34*, 2549.
(13) Chivers, T.; Gao, X.; Parvez, M. *Inorg. Chem.* **1996**, *35*, 4336.
(14) Schatte, G.; Chivers, T.; Jaska, C.; Sandblom, N. *Chem. Commun.* **2000**, 1657.
(15) Chivers, T.; Parvez, M.; Schatte, G. *Angew. Chem., Int. Ed.* **1999**, *38*, 2217.
(16) Chivers, T.; Parvez, M.; Schatte, G. *Inorg. Chem.* **1999**, *38*, 5171.
(17) Chivers, T.; Parvez, M.; Schatte, G. *Inorg. Chem.* **2001**, *40*, 540.
(18) Svensson, P. H.; Kloo, L. *Chem. Rev.* **2003**, *103*, 1649.
(19) Chivers, T.; Enright, G.; Sandblom, N.; Schatte, G.; Parvez, M. *Inorg. Chem.* **1999**, *38*, 5431.
(20) Chivers, T.; Sandblom, N.; Schatte, G. *Inorg. Synth.* **2004**, *34*, 42.

Preparation of 4a. A solution of HCF_3SO_3 (0.075 g, 0.50 mmol) in toluene (15 mL) was added slowly to an orange-yellow solution of **1** (0.270 g, 0.50 mmol) in toluene (20 mL) cooled to −80 °C. The reaction mixture was stirred for 1 h at −80 °C and then for 3 h at 23 °C. The solvent was evaporated under a vacuum to give **4a** as a yellow powder (0.324 g, 94%). Pale yellow plates were grown from CH_3CN at −20 °C in 2 weeks. ^{1}H NMR (d_8-toluene): δ 4.10 (1H, $\nu_{1/2}$ 14.8 Hz, N*H*), 1.44 [18H, $\nu_{1/2}$ 1.4 Hz, C(CH_3)$_3$, endocyclic N^{t}Bu groups], 1.19 [18H, $\nu_{1/2}$ 42.8 Hz, C(CH_3)$_3$, exocyclic N^{t}Bu groups]. ^{13}C{^{1}H} NMR (d_8-toluene): δ 58.8 [*C*(CH$_3$)$_3$], 35.62 [C(*C*H$_3$)$_3$, endocyclic N^{t}Bu groups], 34.4 [C(*C*H$_3$)$_3$, exocyclic N^{t}Bu groups]. ^{125}Te NMR (d_8-toluene): δ 1455 (s, $\nu_{1/2}$ ∼2800 Hz). IR (cm^{-1}): 3299 [υ(N−H)]. Anal. Calcd for $C_{17}H_{37}F_3N_4O_3STe_2$: C, 29.60; H, 5.42; N, 8.12. Found: C, 29.23; H, 5.31; N, 7.95.

Reaction of 4a with LiI and I_2. A mixture of LiI (0.040 g, 0.30 mmol) and I_2 (0.343 g, 1.35 mmol) in CH_2Cl_2 (30 mL) was cooled to −80 °C. A solution of **4a** (0.207 g, 0.30 mmol) in CH_2Cl_2 (40 mL) was added slowly via cannula. The reaction mixture was stirred for 0.5 h at −80 °C and then for 2.5 h at 23 °C. The precipitate of Li[CF_3SO_3] (and a small amount of the product) was allowed to settle, and the solution was decanted via cannula. The solvent was evaporated under a vacuum to give **5**[21] as dark red powder (0.313 g). The absence of Li[CF_3SO_3] in the product was confirmed by ^{7}Li NMR spectroscopy. Dark red crystals were obtained from a CH_3CN solution after ca. 48 h at −20 °C. ^{1}H NMR (CD_2Cl_2): δ 9.04 (1H, br, N*H*), 1.65 [18H, C(CH_3)$_3$, endocyclic N^{t}Bu groups], 1.52 [9H, C(CH_3)$_3$, exocyclic N^{t}Bu group], 1.26 [9H, C(CH_3)$_3$, exocyclic N^{t}Bu group]. ^{13}C{^{1}H} NMR (CH_2Cl_2): δ 35.7 [C(*C*H$_3$)$_3$, endocyclic N^{t}Bu groups], 32.9 [C(*C*H$_3$)$_3$, exocyclic N^{t}Bu group], 29.3 [C(*C*H$_3$)$_3$, exocyclic N^{t}Bu group]. ^{125}Te: δ 1560. IR (cm^{-1}): 3275 [υ(N−H)]. Raman (cm^{-1}, %): 92 (12), 118 (18), 140 (25), 168 (62), 181 (100).

Reaction of [(^{t}BuNMe)Te(μ-N^{t}Bu)$_2$TeN^{t}Bu][OSO_2CF_3] with LiI and I_2. A mixture of LiI (0.033 g, 0.25 mmol) and I_2 (0.318 g, 1.25 mmol) in CH_3CN (20 mL) was cooled to −30 °C. A solution of [(^{t}BuNMe)Te(μ-N^{t}Bu)$_2$TeN^{t}Bu][OSO_2CF_3] (0.176 g, 0.25 mmol) in CH_3CN (20 mL) was added slowly via cannula. The reaction mixture was stirred for 0.5 h at −30 °C and then for 3 h at 23 °C. The solvent was evaporated under a vacuum, yielding a dark red powder (0.378 g), which contained Li[CF_3SO_3]. ^{1}H NMR (CD_3CN): δ 3.25 (3H, ^{t}BuNC*H*$_3$), 1.57 [18H, C(CH_3)$_3$, endocyclic N^{t}Bu groups], 1.54 [9H, C(CH_3)$_3$, exocyclic N^{t}Bu group], 1.51 [9H, C(CH_3)$_3$, exocyclic N^{t}Bu group]. ^{13}C{^{1}H} NMR: δ 65.3 [*C*(CH$_3$)$_3$, exocyclic N^{t}Bu group], 63.8 [*C*(CH$_3$)$_3$, endocyclic N^{t}Bu group], 61.2 [*C*(CH$_3$)$_3$, exocyclic N^{t}Bu group], 34.7 [C(*C*H$_3$)$_3$, endocyclic N^{t}Bu group], 32.8 [C(*C*H$_3$)$_3$, exocyclic N^{t}Bu group], 31.8 (^{t}BuN*C*H$_3$), 30.6 [C(*C*H$_3$)$_3$, exocyclic N^{t}Bu group]. ^{125}Te NMR: δ 1587, 1552. Red crystals of **6**·2MeCN were obtained from CH_3CN after 1 h at −20 °C.

Reaction of [(^{t}BuNMe)Te(μ-N^{t}Bu)$_2$Te(MeN^{t}Bu)][OSO_2CF_3]$_2$ with LiI and I_2. A mixture of LiI (0.067 g, 0.50 mmol) and I_2 (0.254 g, 1.00 mmol) in CH_3CN (20 mL) was cooled to −30 °C. A solution of [(^{t}BuNMe)Te(μ-N^{t}Bu)$_2$Te(MeN^{t}Bu)][OSO_2CF_3]$_2$ (0.217 g, 0.25 mmol) in CH_3CN (20 mL) was added slowly via cannula. The reaction mixture was stirred for 0.5 h at −30 °C and then for 3 h at 23 °C. The solvent was evaporated under a vacuum, yielding a dark red powder (0.338 g), which contained Li[CF_3SO_3]. ^{1}H NMR (CD_3CN): δ 3.48 (6H, ^{t}BuNC*H*$_3$), 1.62 [18H, C(CH_3)$_3$], 1.53 [18H, C(CH_3)$_3$]. ^{13}C{^{1}H} NMR: δ 65.3 [*C*(CH$_3$)$_3$], 64.1 [*C*(CH$_3$)$_3$], 34.4 [C(*C*H$_3$)$_3$], 33.6 (^{t}BuN*C*H$_3$), 30.5 [C(*C*H$_3$)$_3$]. ^{125}Te NMR: δ 1586. Red crystals of **6** were obtained from CH_3CN after 24 h at −20 °C.

X-ray Crystallography. Crystals of **3**, **4a,** **5**·2MeCN, **6**, and **6**·2MeCN were coated with Paratone oil and mounted on a CryoLoop. Diffraction data were collected on a Nonius KappaCCD diffractometer using monochromated Mo Kα radiation (λ = 0.71073 Å) at −100 °C. The data sets were corrected for Lorentz and polarization effects, and an empirical absorption correction was applied to the net intensities. The structures were solved by direct methods using SHELXS-97[22] and refined using SHELXL-97.[23] After the full-matrix least-squares refinement of the non-hydrogen atoms with anisotropic thermal parameters, the hydrogen atoms were placed in calculated positions (C−H = 0.98 Å). In the final refinement, the hydrogen atoms were riding with the carbon or nitrogen atom they were bonded to. Hydrogen atoms bonded to nitrogen were located from the difference Fourier maps and refined normally. The isotropic thermal parameters of the hydrogen atoms were fixed at 1.2 times that of the corresponding carbon or nitrogen atom. The scattering factors for the neutral atoms were those incorporated with the programs. Crystallographic data are summarized in Table 1.

The iodine atoms in **5** were disordered. Upon refinement, this disorder was resolved in terms of a mixture of two different species, [(^{t}BuNH)Te(μ-N^{t}Bu)$_2$Te(N^{t}Bu)]$_2$I$_{20}$ (**5a**) and [(^{t}BuNH)Te(μ-N^{t}Bu)$_2$Te(NH^{t}Bu)]$_2$I$_{18}$ (**5b**).[24] During the refinement, the pairs of atoms that overlapped with each other (N4A and N4B, I5A and I5B, I6A and I6B, I7A and I7B, I8A and I8B, and I10A and I10B) were fixed in the same positions, and their thermal parameters were constrained to be equal.

Results and Discussion

Formation and Crystal Structure of 3. The reaction of **1** with elemental iodine (I_2) was conducted in several different molar ratios (1:1, 1:3, 1:5, and 1:10) and afforded highly moisture-sensitive red powders. Single crystals were grown from the CH_3CN solutions for the products of the 1:3 and 1:5 molar-ratio reactions. In both cases, the crystallization procedure gave rise to the partially hydrolyzed product **3**.

The crystal structure of **3,** with the atomic numbering scheme, is shown in Figure 1. Selected bond parameters are summarized in Table 2. The structure is centrosymmetric and contains a dimeric imidotelluroxane dication [(^{t}BuIN)Te(μ-N^{t}Bu)$_2$Te(μ-O)]$_2^{2+}$ and two I_3^- units that are connected by I···I and Te···I secondary interactions. Similarly to the case of imidotelluroxane ligands in the Cu and Ag complexes,[16] the two [(^{t}BuIN)Te(μ-N^{t}Bu)$_2$] fragments in the dication in **3** lie in trans positions with respect to the central Te_2O_2 ring (see Figure 1). The N3−I1 bond length of 2.09(2) Å in the dication is close to the sum of the covalent radii for iodine and nitrogen (2.06 Å).[25] By contrast, the

(21) The product that, upon recrystallization from acetonitrile, was found to be a solid solution of [(^{t}BuNH)Te(μ-N^{t}Bu)$_2$Te(N^{t}Bu)]$_2$I$_{20}$ (**5a**) and [(^{t}BuNH)Te(μ-N^{t}Bu)$_2$Te(NH^{t}Bu)]$_2$I$_{18}$ (**5b**) is referred to as **5**.

(22) Sheldrick, G. M. *SHELXS-97. Program for Crystal Structure Determination*; University of Göttingen: Göttingen, Germany, 1997.

(23) Sheldrick, G. M. *SHELXL-97. Program for Crystal Structure Refinement*; University of Göttingen: Göttingen, Germany, 1997.

(24) The iodine atoms in the I_{20} fragment of **5a** are denoted as I1A−I10A, and those in the I_{18} fragment of **5b** are denoted as I2B and I2B−I10B. The pairs of atoms I6A and I6B, I7A and I7B, I8A and I8B, and I10A and I10B coincide, their thermal displacement factors are constrained to be equal, and they are fixed in the same positions.

(25) Boucher, M.; Macikenas, D.; Ren, T.; Protasiewicz, J. D. *J. Am. Chem. Soc.* **1997**, *119*, 9366.

Table 1. Crystal Data and Structure Refinement for **3**, **4a**, **5**·2MeCN, **6**, and **6**·2MeCN[a]

	3	**4a**	**5**·2MeCN	**6**	**6**·2MeCN
empirical formula	$C_{12}H_{27}N_3OTe_2I_4$	$C_{17}H_{37}N_4O_3F_3STe_2$	$C_{18}H_{40.11}N_5Te_2I_{9.89}$	$C_{13}H_{30}N_3OTe_2I_3$	$C_{15}H_{33}N_4OTe_2I_3$
fw	992.17	689.77	1836.27	880.30	921.35
cryst syst	monoclinic	orthorhombic	triclinic	triclinic	monoclinic
space group	$P2_1/n$	$P2_12_12_1$	$P-1$	$P-1$	$P2_1/n$
a, Å	9.113(2)	16.183(3)	10.332(2)	9.943(2)	12.179(2)
b, Å	18.516(4)	17.695(4)	13.185(3)	9.957(2)	15.674(1)
c, Å	15.918(3)	18.374(4)	17.050(3)	12.931(3)	14.360(3)
α, deg			91.75(3)	104.44(3)	
β, deg	105.33(3)		105.24(3)	101.61(3)	93.90(3)
γ, deg			102.45(3)	93.68(3)	
V, Å^3	2590.3(9)	5262(2)	2178.9(8)	1205.5(4)	2734.9(8)
Z	4	8	2	2	4
T, °C	173(2)	173(2)	173(2)	173(2)	173(2)
ρ_{calcd}, g/cm^3	2.544	1.742	2.799	2.425	2.238
μ(Mo Kα), mm^{-1}	7.024	2.342	8.358	6.266	5.531
cryst size, mm^3	0.13 × 0.05 × 0.05	0.16 × 0.12 × 0.08	0.16 × 0.14 × 0.08	0.10 × 0.10 × 0.05	0.15 × 0.15 × 0.10
F(000)	1776	2704	1622	800	1688
Θ range, deg	2.57−23.25	1.71−26.00	1.24−26.00	2.81−26.00	3.46−26.00
reflns collected	12880	10063	15510	8477	19376
unique reflns	3698	10063	8420	4709	5358
R_{int}	0.1048		0.0324	0.0360	0.0320
R_1 [$I>2\sigma\sigma(I)$][b]	0.0850	0.0404	0.0405	0.0306	0.0254
wR_2 (all data)[c]	0.2168	0.0710	0.0857	0.0659	0.0620
GOF on F^2	1.114	0.997	1.116	0.978	1.047

[a] λ (MoK±) = 0.71073 Å; T = 173(2) K. [b] $R_1 = \sum||F_o| - |F_c||/\sum|F_o|$. [c] $wR_2 = [\sum w(F_o^2 - F_c^2)^2/\sum wF_o^4]^{1/2}$.

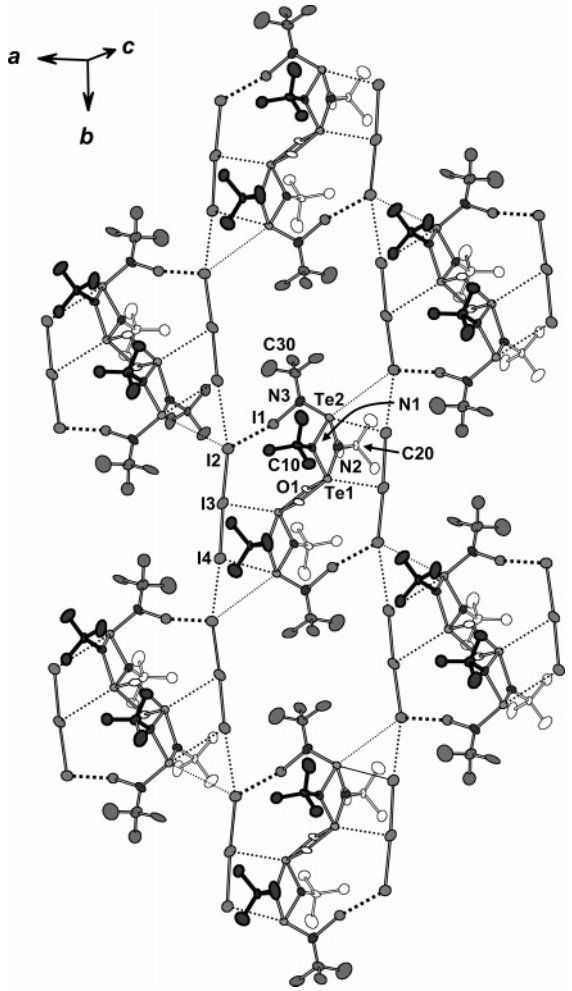

Figure 1. Crystal structure of **3** with the atomic numbering scheme, indicating the I···I close contacts. Thermal ellipsoids are indicated at the 50% probability level. The hydrogen atoms are omitted for clarity.

ionic N···I interactions in $\{[(C_6H_5N)_2(\mu\text{-}I^+)](BF_4)^-\}$ and $[(C_6H_5N)ICl]$ span distances of 2.255(3)−2.261(3) Å[26] and 2.29(1) Å,[27] respectively. The structure also exhibits a secondary I···I interaction [I1···I2 = 3.278(4) Å] and two Te···I close contacts that link the I_3^- ions with the dication [Te2···I4 3.663(3) Å and Te1···I3 3.926(3) Å]. The I···I close contacts between the I_3^- units give rise to infinite polyiodide chains (see Figure 1).

The ^{1}H NMR spectra of the products in CD_3CN revealed small differences in the resonances for the N^{t}Bu groups. For the 1:1 and 1:3 reactions, two equally intense resonances were observed at ca. 1.58 and 1.47 ppm. In the case of the 1:5 reaction, three resonances were observed at 1.58, 1.57, and 1.47 ppm with a respective intensity ratio of 2:1:1. In the case of the 1:10 reaction, the resonances at 1.58 and 1.47 ppm showed an intensity ratio of 3:1.

Because the ^{1}H NMR spectra of the crude reaction products do not exhibit the two resonances in a ratio of 2:1, which is expected for the endocyclic and exocyclic N^{t}Bu groups of the dication $[(^t\text{BuIN})\text{Te}(\mu\text{-N}^t\text{Bu})_2\text{Te}(\mu\text{-O})]_2^{2+}$ (vide supra), hydrolysis must occur only during the recrystallization process. This behavior is reminiscent of our observations for the coordination of **1** to coinage metals.[16] The recrystallization of Ag(I) or Cu(I) complexes of **1** produces the neutral imidotelluroxane $[(^t\text{BuN})\text{Te}(\mu\text{-N}^t\text{Bu})_2\text{Te}(\mu\text{-O})]_2$, which is coordinated to the metal centers by the terminal N^{t}Bu group. The iodine atom that is bonded to nitrogen in **3** fulfils the function of the metal center. We propose that the initial oxidation of **1** by 3 or 5 equiv of I_2 gives rise to an imidotellurium cation containing a covalent N−I bond and a polyiodide (Scheme 1). The subsequent hydrolysis of the terminal ylidic $^t\text{BuN}^--\text{Te}^+$ bond during the recrystallization procedure generates **3**.

Synthesis and Crystal Structure of 4a. In view of the observed generation of polyiodide chains by the imidotelluroxane dication in **3**, the investigation was broadened to include the determination of the templating effect of proto-

(26) Alvarez-Rua, C.; Garcia-Granda, S.; Ballesteros, A.; Gonzales-Bobes, F.; Gonzales, J. M. *Acta Crystallogr., Sect. E* **2002**, *58*, o1381.
(27) Romming, C. *Acta Chem. Scand.* **1972**, *26*, 1555.

Scheme 1

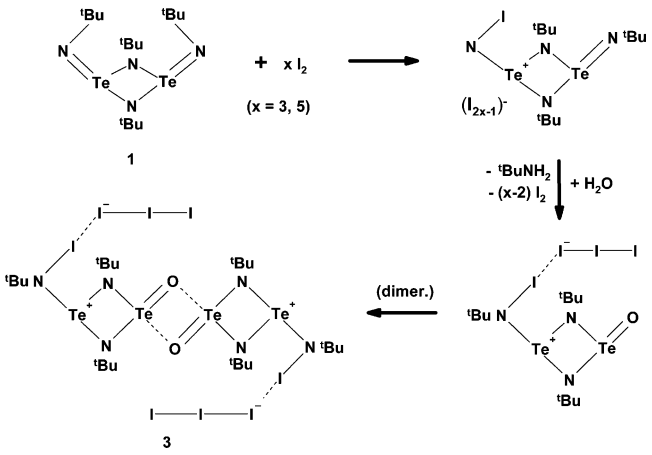

nated and methylated derivatives of **1** on polyiodide formation. We have previously reported that [(ᵗBuNH)Te(*μ*-N^{t}Bu)$_2$Te(N^{t}Bu)]Cl (**4b**), the monoprotonated derivative of **1**, is formed in the reaction of ᵗBuNHLi with $TeCl_4$ in a 7:2 molar ratio in toluene.[2] However, the separation of other products from this chloride salt is difficult and time-consuming. Consequently, we have now investigated the protonation of **1** with HCF_3SO_3, which produces the triflate salt **4a** in quantitative yields (eq 1). This product may be used without further purification.

$$[(^t\text{BuN})\text{Te}(\mu\text{-N}^t\text{Bu})_2\text{Te}(\text{N}^t\text{Bu})] + \text{HCF}_3\text{SO}_3 \rightarrow [(^t\text{BuNH})\text{Te}(\mu\text{-N}^t\text{Bu})_2\text{Te}(\text{N}^t\text{Bu})][\text{OSO}_2\text{CF}_3] \quad (1)$$

4a

The crystal structure of **4a**, and the atomic numbering scheme, is shown in Figure 2. The unit cell of **4a** contains two independent ion pairs. Bond lengths and bond angles for **4a** are compared with those of the chloride salt **4b** in Table 2. As found for **4b**, the protonated cation in **4a** exhibits significantly different exocyclic Te−N bond lengths. The shorter bond length (mean value = ca. 1.86 Å) is only slightly longer than the estimated value of 1.83 Å for a Te(IV)═N double bond.[28,29] The effect of the protonation of **1** is also evident in the bridging Te−N bond distances. The bonds closer to the exocyclic Te═N double bond are ca. 0.12 Å longer than the bonds adjacent to the exocyclic Te−N single bond. This disparity is similar to that reported previously for **4b**.[2]

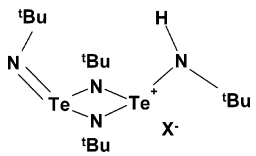

4a, X$^-$ = $CF_3O_2SO^-$
4b, X$^-$ = Cl^-

Similarly to **4b,** the exocyclic N^{t}Bu groups in **4a** show a *cis-endo,exo* arrangement with respect to the Te_2N_2 ring, whereas the N^{t}Bu groups in **1** lie in a *cis-endo,endo* orientation. These different orientations are reflected in a reduction in the N_{endo}−Te−N_{exo} bond angle from ca. 113° in **1** to ca. 100° for the N_{endo}−Te−N_{exo}(H) bond angle in **4a** (see Table 2).

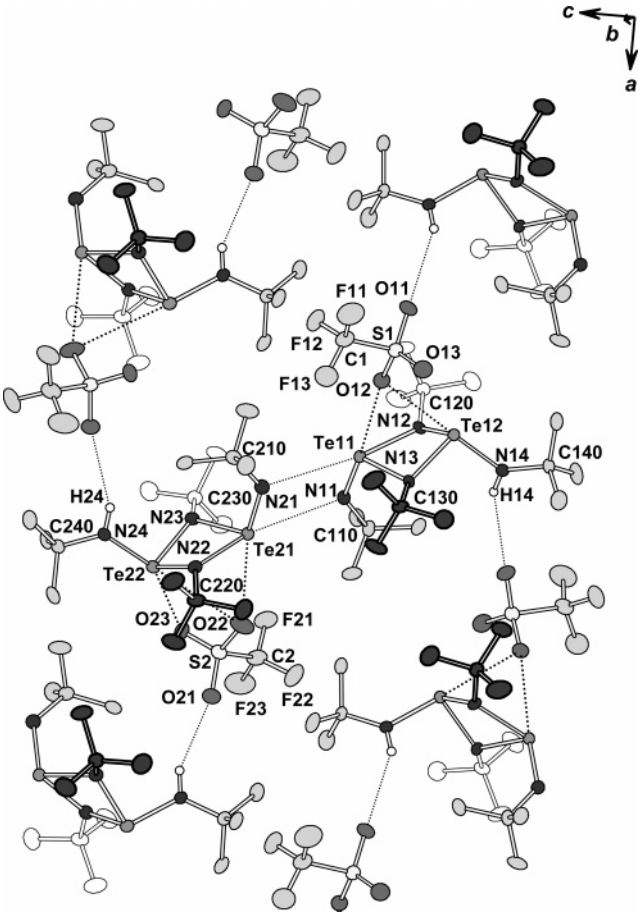

Figure 2. Crystal structure of **4a** with the atomic numbering scheme. Thermal ellipsoids are drawn at the 30% probability level. The hydrogen atoms are omitted for clarity.

One of the two molecules in the asymmetric unit of **4a** exhibits two Te···OSO_2CF_3 close contacts [Te11···O12 = 3.216(5) Å and Te12···O12 = 2.941(5) Å]. The second molecule shows three close contacts [Te21···O22 = 3.202(5) Å, Te22···O22 = 3.357(5) Å, and Te22···O23 = 3.182(6) Å] that are less than the sum of the van der Waals radii for oxygen and tellurium (3.6 Å).[30] The two triflate anions are also linked with the cations by hydrogen bonding [H14···O11 = 2.84(7) and H24···O21 = 2.89(7) Å; ∠N14−H14···O11 = 146(6)° and ∠N24−H24···O21 = 151(6)°]. The two [(ᵗBuNH)Te(*μ*-N^{t}Bu)$_2$Te(N^{t}Bu)]$^+$ cations in the asymmetric unit also show weak Te···N interactions, with values of 3.445(5) and 3.506(5) Å.

NMR Spectra of 4a. We have shown previously that the chloride salt **4b** is fluxional in solution as a result of rapid 1,3 proton shifts between terminal and bridging nitrogen atoms.[13] This fluxionality is readily evident in the 298 K ^{1}H NMR spectrum of **4b**, in which only a single resonance at 1.63 ppm is observed for the N^{t}Bu groups. By contrast, the

(28) Munzenberg, J.; Roesky, H. W.; Noltemeyer, M.; Besser, S.; Herbst-Irmer, R. *Z. Naturforsch.* **1993**, *48b*, 199.
(29) Leichtweis, I.; Hasselbrink, R.; Roesky, H. W.; Noltemeyer, M.; Herzog, A. *Z. Naturforsch.* **1993**, *48b*, 1234.
(30) Emsley, J. *The Elements*, 3rd ed.; Clarendon Press: Oxford, U.K., 1998.

Table 2. Selected Bond Lengths (Å) and Angles (deg) in **3**, **4a**, **5a**, **5b**, **6**, and **6**·2MeCN

$[(^t\text{BuIN})\text{Te}(\mu\text{-N}^t\text{Bu})_2\text{Te}(\mu\text{-O})]_2(\text{I}_3)_2$ (**3**)

Te1−N1	2.02(2)	Te2−N3	1.98(2)	I1−I2	3.278(4)	Te2···I2[b]	4.174(3)
Te1−N2	2.07(2)	Te1−O1	1.88(2)	I2−I3	2.916(3)	Te2···I4[a]	3.663(3)
Te2−N1	1.99(2)	Te1−O1[a]	2.08(2)	I3−I4	2.887(3)	I2···I4[c]	3.576(3)
Te2−N2	1.96(2)	N3−I1	2.09(2)	Te1···I3[a]	3.926(3)		
N1−Te2−N2	76.9(9)	N1−Te2−N3	101.6(10)	N2−Te1−O1	87.4(7)	I1−I2−I3	108.91(9)
N1−Te1−N2	73.7(8)	N2−Te2−N3	102.4(9)	N2−Te1−O1[a]	150.5(8)	I2−I3−I4	176.5(1)
Te1−N1−Te2	103.9(9)	N1−Te1−O1	111.3(8)	Te2−N3−I1	120.9(12)	N3−Te2−Te1	113.2(7)
Te1−N2−Te2	103.0(9)	N1−Te1−O1[a]	90.3(8)	N3−I1−I2	169.2(6)	Te1−Te1−Te2[a]	125.83(9)

$[(^t\text{BuNH})\text{Te}(\mu\text{-N}^t\text{Bu})_2\text{Te}(\text{N}^t\text{Bu})]\text{X}$ {X = OSO_2CF_3 (**4a**), Cl (**4b**)}

	4a[d]		**4b**[e]		**4a**[d]		**4b**[e]
	(*n* = 1)	(*n* = 2)			(*n* = 1)	(*n* = 2)	
Te*n*1−N*n*1	1.854(5)	1.870(5)	1.840(9)	Te*n*1···O*n*2	3.216(5)[f]	3.202(5)[g]	
Te*n*1−N*n*2	2.103(5)	2.082(5)	2.092(10)	Te*n*2···O*n*2	2.941(5)[f]	3.357(5)[g]	
Te*n*1−N*n*3	2.104(5)	2.123(5)	2.112(8)	Te*n*2···O*n*3	3.766(6)[f]	3.182(6)[g]	
Te*n*2−N*n*2	1.988(5)	1.977(5)	2.003(8)	N*n*4−H*n*4	0.79(7)	0.84(6)	
Te*n*2−N*n*3	1.985(4)	1.975(5)	2.00(1)	H*n*4···O*n*1	2.84(7)	2.89(7)	
Te*n*2−N*n*4	1.952(6)	1.974(6)	1.980(9)				
N*n*1−Te*n*1−N*n*2	109.6(2)	109.4(2)	108.2(4)	N*n*4−H*n*4···O*n*1	146(6)	151(6)	
N*n*1−Te*n*1−N*n*3	110.6(2)	110.6(2)	109.7(4)	N*n*3−Te*n*2−N*n*4	98.6(2)	100.0(2)	95.2(4)
N*n*2−Te*n*1−N*n*3	72.2(2)	72.9(2)	73.0(3)	Te*n*1−N*n*2−Te*n*2	100.7(2)	101.9(2)	100.1(4)
N*n*2−Te*n*2−N*n*3	77.2(2)	78.5(2)	77.4(4)	Te*n*1−N*n*3−Te*n*2	100.7(2)	100.5(2)	99.5(4)
N*n*2−Te*n*2−N*n*4	100.5(2)	100.4(2)	95.5(4)				

$[(^t\text{BuNH})\text{Te}(\mu\text{-N}^t\text{Bu})_2\text{Te}\{\text{N}(\text{I}_2)_2{}^t\text{Bu}\}]_2(\text{I}_3^-)_2(\text{I}_2)_3$ (**5a**) and $[(^t\text{BuNH})\text{Te}(\mu\text{-N}^t\text{Bu})_2\text{Te}(\text{NH}^t\text{Bu})]_2(\text{I}_3)_4(\text{I}_2)_3$ (**5b**)
common bond lengths and angles in **5a** and **5b**[h]

Te1−N1	1.923(6)	Te2−N2	2.009(6)	I6(A,B)−I7(A,B)[i]	3.427(1)	I10(A,B)−I10(A,B)[i,j]	2.743(1)
Te1−N2	2.013(6)	Te2−N3	2.030(6)	I7(A,B)−I8(A,B)[i]	3.113(1)	I7(A,B)−I10(A,B)−I10(A,B)[i,j]	173.65(4)
Te1−N3	2.018(6)	Te2−N4(A,B)[i]	1.943(6)	I7(A,B)−I10(A,B)[i]	3.431(1)	I6(A,B)−I7(A,B)−10(A,B)[i]	75.62(3)
N1−Te1−N2	98.5(3)	N2−Te2−N3	74.9(2)	Te1−N2−Te2	101.5(3)		
N1−Te1−N3	96.5(3)	N2−Te2−N4(A,B)[i]	98.8(3)	Te1−N3−Te2	100.6(3)		
N2−Te1−N3	75.1(2)	N3−Te2−N4(A,B)[i]	99.8(3)	I6(A,B)−I7(A,B)−I8(A,B)[i]	84.71(3)		

5a		**5b**		**5a**		**5b**	
N4A−I1A	2.131(7)			I3A−I4A	2.788(2)	I3B−I4B	2.77(1)
I1A−I2A	3.118(1)			I5A−I6A	2.736(2)	I5B−I6B	2.743(9)
I2A−I3A	3.095(2)	I2B−I3B	3.06(2)	I8A−I9A	2.792(2)	I8B−I9B	2.76(2)
I2A−I5A	3.503(2)	I2B−I5B	3.51(1)				
N4A−I1A−I2A	173.0(1)			I3A−I2A−I5A	86.08(5)	I3B−I2B−I5B	84.0(4)
I1A−I2A−I3A	84.75(4)			I5A−I6A−I7A	172.76(4)	I5B−I6B−I7B	170.8(4)
I1A−I2A−I5A	81.92(4)			I7A−I8A−I9A	176.97(9)	I7B−I8B−I9B	172.0(4)
I2A−I3A−I4A	174.99(8)	I2B−I3B−I4B	169.6(6)				

$[(^t\text{BuMeN})\text{Te}(\mu\text{-N}^t\text{Bu})_2\text{Te}(\mu\text{-O})]_2(\text{I}_3)_2$ (**6**) and $[(^t\text{BuMeN})\text{Te}(\mu\text{-N}^t\text{Bu})_2\text{Te}(\mu\text{-O})]_2(\text{I}_3)_2$·2MeCN (**6**·2MeCN)

	6	**6**·2MeCN		**6**	**6**·2MeCN		**6**	**6**·2MeCN
Te1−N1	2.012(4)	2.026(3)	Te1−O1	1.911(4)	1.908(3)	Te1···I3		3.8647(7)[n]
Te1−N2	2.110(4)	2.090(3)	Te1−O1	2.107(3)[k]	2.105(2)[l]	Te2···I1	3.747(1)[m]	3.7057(9)
Te2−N1	2.005(4)	2.006(3)	I1−I2	3.0098(9)	2.9943(9)	Te2···I2	3.842(1)[m]	3.8836(7)
Te2−N2	1.959(4)	1.948(3)	I2−I3	2.8538(9)	2.8467(9)	I1···I3		4.039(1)[n]
Te2−N3	1.967(4)	1.962(3)	Te1···I1	4.015(1)	4.0089(7)[l]			
N1−Te2−N2	77.9(2)	77.8(1)	N2−Te2−N3	99.2(2)	100.4(1)	N2−Te1−O1	151.3(2)[k]	151.3(1)[l]
N1−Te1−N2	74.3(2)	74.2(1)	N1−Te1−O1	108.2(2)	108.0(1)	I1−I2−I3	177.74(2)	178.98(1)
Te1−N1−Te2	104.3(2)	101.9(1)	N1−Te1−O1	89.3(2)[k]	89.5(1)[l]	Te1−Te1−Te2	121.87(3)[k]	126.52(1)[l]
Te1−N2−Te2	102.4(2)	101.6(1)	N2−Te1−O1	86.9(2)	86.4(1)			
N1−Te2−N3	100.0(2)	100.2(1)	N3−Te2−Te1	107.5(1)	113.78(9)			

[a] Symmetry operation: $-x, -y, -z + 1$. [b] Symmetry operation: $x - 0.5, -y + 0.5, z + 0.5$. [c] Symmetry operation: $-x - 0.5, y + 0.5, -z + 1.5$. [d] There are two independent molecules in the asymmetric unit, the bond parameters of which are distinguished by the index *n*. [e] The data of **4b** have been taken from ref 2. The atoms have been renumbered to correspond those of **4a**. Because there is only one molecule in the asymmetric unit, the index *n* can be omitted. [f] The symmetry operation of O1*i* (*i* = 2, 3): $x - 0.5, 1.5 - y, -z$. [g] The symmetry operation of O2*i* (*i* = 2, 3): $x + 0.5, 1.5 - y, 1 -$ z. [h] The set of atoms in the disordered structure belonging to **5a** have been denoted by a label A, and those belonging to **5b** have been denoted by a label B. [i] The atoms A and B have been constrained in the same position. [j] Symmetry operation: $2 - x, 1 - y, 2 - z$. [k] The symmetry operations used to generate the last atom: $-x, -y + 1, -z + 1$. [l] The symmetry operations used to generate the last atom: $-x + 1, -y, -z$. [m] The symmetry operations used to generate the last atom: $-x + 1, -y + 1, -z + 1$. [n] The symmetry operations used to generate the last atom: $x - 0.5, -y + 0.5, z + 0.5$.

^{1}H NMR spectrum of **4a** in toluene at 298 K shows two equally intense resonances at 1.44 and 1.19 ppm, in addition to the broad resonance at 4.10 ppm attributed to the NH proton. The broad singlet at 1.19 ppm ($\nu_{1/2}$ = 42.8 Hz) is tentatively assigned to the protons of the exocyclic N^{t}Bu groups and the singlet at 1.44 ppm ($\nu_{1/2}$ = 1.4 Hz) to the protons of the endocyclic N^{t}Bu groups. The ^{1}H NMR spectra in the temperature range 193−273 K support this assignment by revealing the splitting of the resonance at 1.19 ppm into two resonances at 1.08 and 1.42 ppm at 213 K. Concomitantly, the singlet at 1.44 ppm is shifted to 1.59 ppm. At this temperature, the ^{1}H NMR spectrum of **4a** shows the

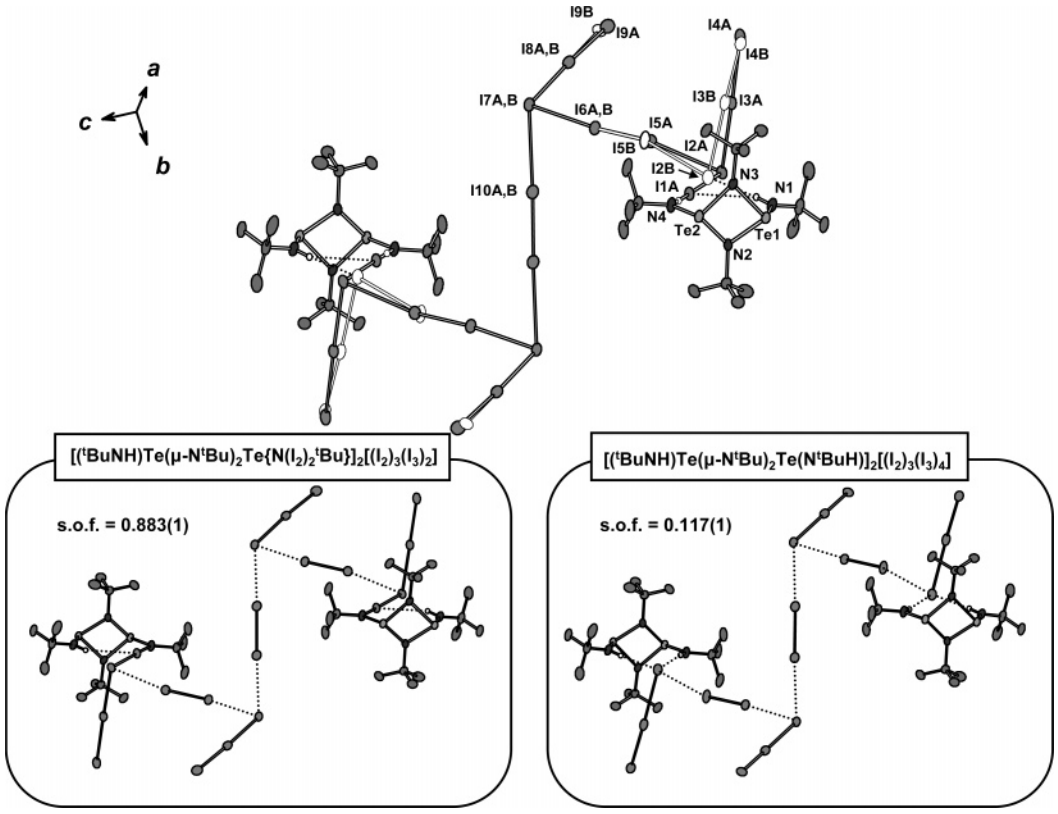

Figure 3. Disordered crystal structure containing **5a**·2MeCN and **5b**·2MeCN with the atomic numbering scheme. The disorder has been resolved in terms of 88.3(1)% of $[(^t\text{BuNH})\text{Te}(\mu\text{-N}^t\text{Bu})_2\text{Te}\{\text{N}(\text{I}_2)_2{}^t\text{Bu}\}]_2(\text{I}_3)_2(\text{I}_2)_3\cdot 2\text{MeCN}$ (**5a**·2MeCN; atom set A) and 11.7(1)% of $[(^t\text{BuNH})\text{Te}(\mu\text{-N}^t\text{Bu})_2\text{Te}\{\text{NH}^t\text{Bu}\}]_2(\text{I}_3)_4(\text{I}_2)_3\cdot 2\text{MeCN}$ (**5b**·2MeCN; atom set B). Thermal ellipsoids are drawn at the 50% probability level. The hydrogen atoms and solvent molecules are omitted for clarity.

expected three resonances for the inequivalent N^{t}Bu groups in the approximate intensity ratio of 2:1:1, suggesting that **4a** exhibits fluxional behavior similar to that discussed previously for **4b**.[13] Consistently, the ^{13}C NMR spectrum of **4a** shows two resonances at 35.6 and 34.4 ppm at 296 K. The latter resonance is resolved into two broad resonances at 213 K. However, only one resonance is discerned at 58.8 ppm in the region expected for the α carbon of the ^{t}Bu groups. The ^{125}Te NMR spectrum of **4a** at 298 K shows a very broad resonance at ca. 1455 ppm (cf. 1475 ppm for **1**).[16]

Formation and Crystal Structures of 5a and 5b. The reaction of **4a** with LiI and I_2 in the molar ratio 1:1:4.5 yields a product that, upon recrystallization from CH_3CN, produces a solid solution containing **5a** and **5b**.[31] The crystal structure is disordered.[32] The atomic numbering scheme is shown in Figure 3. The structure is centrosymmetric, with the asymmetric unit containing half of the molecular species. The other half is completed by symmetry.

The resolution of the disorder of **5**·2MeCN into **5a**·2MeCN and **5b**·2MeCN is also indicated in Figure 3. The refinement of site occupation factors shows that the abundance of **5a** in the lattice is 88.3(1)%, and that of **5b** is 11.7(1)%. Selected bond lengths and angles of both **5a** and **5b** are presented in Table 2.

It can be deduced by consideration of the bond distances that $[(^t\text{BuNH})\text{Te}(\mu\text{-N}^t\text{Bu})_2\text{Te}(\text{N}^t\text{Bu})]_2\text{I}_{20}$ (**5a**) can be formulated as $[(^t\text{BuNH})\text{Te}(\mu\text{-N}^t\text{Bu})_2\text{Te}\{\text{N}(\text{I}_2)_2{}^t\text{Bu}\}]_2(\text{I}_3)_2(\text{I}_2)_3$ containing two $[(^t\text{BuNH})\text{Te}(\mu\text{-N}^t\text{Bu})_2\text{Te}\{\text{N}(\text{I}_2)_2{}^t\text{Bu}\}]^+$ cations. The I_{20} framework involves two N−I−I−I−I units, two I_3^- ions, and three I_2 molecules. The bonding in the N−I_4 fragment is similar to that in 2-imidazolidinethione bis(diiodine),[33] 2-imidazolidinethione tris(diiodine),[33] and [*N*-methylbenzothiazole-2(3H)-selenone]bis(diiodine)[34] and can be interpreted in terms of the formation of a charge-transfer interaction, as indicated in Figure 4. The donation of the lone-pair electron density to the σ^* orbital (lowest unoccupied molecular orbital) of an I_2 molecule with the simultaneous transfer of electron density from the σ^* (highest occupied molecular orbital) orbital of this I_2 molecule to the σ^* of a second I_2 molecule explains the formation of a relatively short N4A−I1A bond [2.131(7) Å], the lengthening of the I1A−I2A bond [3.118(1) Å] compared to the I−I single bond in free I_2,[35] the formation of the I2A−I3A interaction [3.095(2) Å], and the slight lengthening of the I3A−I4A bond [2.788(2) Å] of the second I_2. The bond angle I1A−I2A−I3A of 84.75(4)° is also consistent with the interaction shown in Figure 4.

A comparison with relevant E−I (E = N, S, or Se) and I−I bond lengths in the E−I1−I2−I3−I4 fragments of **3**, **5a,** 2-imidazolidinethione bis(diiodine), 2-imidazolidine-

(31) The initial reaction was carried out in CH_2Cl_2. The insoluble byproduct $\text{Li}[CF_3SO_3]$ was removed by decantation of the solution.
(32) The formation of the disordered solid solution of **5a**·2MeCN and **5b**·2MeCN could be carried out reproducibly.
(33) Herbstein, F. H.; Schwotzer, W. *J. Am. Chem. Soc.* **1984**, *106*, 2367.
(34) Cristiani, F.; Demartin, F.; Devillanova, F. A.; Isaia, F.; Lippolis, V.; Verani, G. *Inorg. Chem.* **1994**, *33*, 6315.

Table 3. Comparison of the Bond Parameters in the E−I1−I2−I3−I4 (E = N, S, Se) Fragments in **3**, **5a**, $(CH_2)_2N_2C{=}SI_4$, $(CH_2)_2N_2C{=}SI_6$, and $C_6H_4N(Me)SC{=}SeI_4$ (for Numbering of Iodine Atoms, See Figure 4)

compound	E−I1 (Å)	I1−I2 (Å)	I2−I3 (Å)	I3−I4 (Å)	∠E−I1−I2 (deg)	∠I1−I2−I3 (deg)	∠I2−I3−I4 (deg)
3	2.09(2)	3.278(4)	2.916(3)	2.887(3)	169.2(6)	108.91(9)	176.5(1)
5a	2.132(7)	3.118(1)	3.095(2)	2.788(2)	173.0(1)	84.75(4)	174.99(8)
$(CH_2)_2N_2C{=}SI_4$[a]	2.487(3)	3.147(1)	3.004(1)	2.851(1)	177.9(1)	92.4(4)	177.1(1)
$(CH_2)_2N_2C{=}SI_6$[a]	2.580(1)	2.984(1)	3.472(1)	2.760(1)	177.5(1)	85.1(4)	177.7(1)
$C_6H_4N(Me)SC{=}SeI_4$[b]							
molecule 1	2.639(1)	3.071(1)	3.155(1)	2.746(1)	176.66(3)	85.46(2)	178.25(3)
molecule 2	2.662(1)	3.059(1)	3.341(1)	2.762(1)	178.84(3)	117.99(2)	173.27(3)
molecule 3	2.720(1)	2.960(1)	3.380(1)	2.764(1)	171.52(3)	108.99(2)	176.48(3)

[a] ref 33. [b] ref 34.

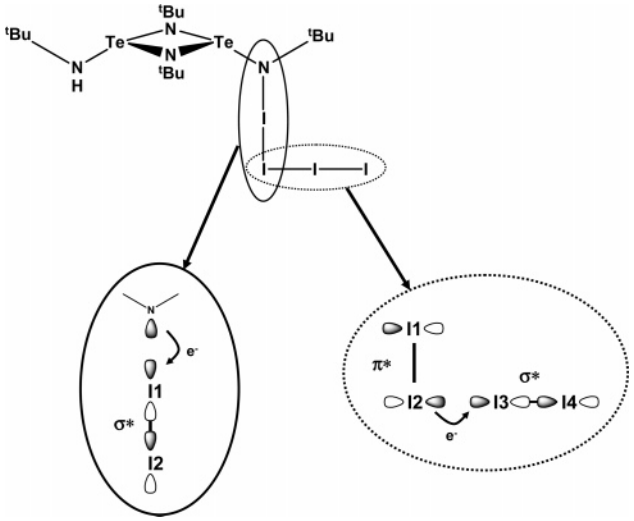

Figure 4. lp(N) → $\sigma^*(I_2)$ and $\pi^*(I_2)$ → $\sigma^*(I_2)$ interactions giving rise to the N−I−I−I−I charge-transfer bonding in **5a**.

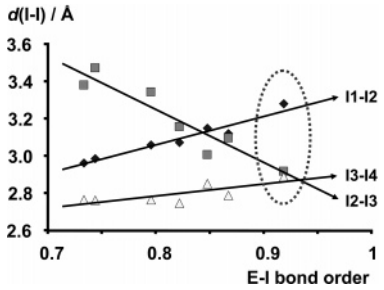

Figure 5. Trends in the bond lengths in the E−I−I−I−I (E = N, S, Se) fragment of **3**, **5a**, $(CH_2)_2N_2C{=}SI_4$,[33] $(CH_2)_2N_2C{=}SI_6$,[33] and $C_6H_4N(Me)SC{=}SeI_4$[34] as a function of the strength of the E−I1 interaction.[36] The arrows in the figure do not indicate linear relationships but serve to assist the visualization of the trends. The bond parameters of **3** are indicated by an ellipse.

thione tris(diiodine), and [*N*-methylbenzothiazole-2(3H)-selenone]bis(diiodine) (see Table 3) provides further support for the formation of this kind of charge-transfer interaction. Figure 5 illustrates that all three I−I bonds exhibit the expected trends as a function of the E−I interaction. As the strength of the E−I1 interaction grows,[36] the I1−I2 bond becomes longer, the I2−I3 bond becomes shorter, and the I3−I4 bond becomes longer. It can also be concluded from Figure 5 that, whereas **5a**, 2-imidazolidinethione bis(diiodine), and [*N*-methylbenzothiazole-2(3H)-selenone]bis(diiodine) can be considered to exhibit E−I charge-transfer interactions of varying strengths, **3** is best described in terms of an ion pair containing the $[(^t\text{BuIN})\text{Te}(\mu\text{-N}^t\text{Bu})_2\text{Te}(\mu\text{-O})]_2^{2+}$ dication and two I_3^- anions, as depicted in Scheme 1.[38] The more open ∠I1−I2−I3 bond angle in **3**, compared to those in other species shown in Table 3, also indicates the nondirectional character of the E−I1 interaction in **3**.

There are two symmetry-related I_3^- ions in the I_{20} framework. They are approximately linear [∠I7A−I8A−I9A = 176.97(9)°]. The two I−I bonds of 3.113(1) (I7A−I8A) and 2.792(2) Å (I8A−I9A) are typical for the asymmetric I_3^- ions.[18] The two independent I_2 units show bond lengths of 2.736(2) and 2.743(1) Å (I5A−I6A and I10A−I10A*, respectively; I10A* has been generated from I10A by the symmetry operation $2 - x$, $1 - y$, $2 - z$) and are close to I−I single bond lengths.[35] The NI_4, I_3^-, and I_2 units of the I_{20} framework in **5a** are linked together by I···I secondary bonding interactions that span a narrow range of 3.427(1)−3.503(2) Å.

The bonding arrangement in **5b** is somewhat simpler. The species can be formulated as $[(^t\text{BuNH})\text{Te}(\mu\text{-N}^t\text{Bu})_2\text{Te}(\text{NH}^t\text{Bu})]_2(I_3)_4(I_2)_3$. The $[(^t\text{BuNH})\text{Te}(\mu\text{-N}^t\text{Bu})_2\text{Te}(\text{NH}^t\text{Bu})]^{2+}$ cation is linked to an I_3^- anion by two N4B−H4B···I1B hydrogen bonds [H1···I2B = 2.823(5) Å, ∠N1−H1···I2B = 172.1(4)°; H4B···I1B = 2.984(6) Å, ∠N4B−H4B···I1B = 171.5(5)°]. In the I_{18} framework of **5b**, there are four I_3^- anions, two of which are independent and two of which are generated from them by symmetry. Their bond parameters are also characteristic for I_3^- anions.[18] The I−I bonds in the I_2 units of **5b** show identical values to those in **5a** because of the overlap of the corresponding iodine atoms.

The possibilities for the packing of **5a** and **5b** in the crystal lattice are shown in Figure 6. Because the site occupancy of **5a** is 88.3(1)% and that of **5b** is 11.7(1)%, there is a probability of 78% that two $[(^t\text{BuNH})\text{Te}(\mu\text{-N}^t\text{Bu})_2\text{Te}\{\text{N}(I_2)_2{}^t\text{Bu}\}]_2(I_3)_2(I_2)_3$ units share adjacent positions in the lattice. The probability of one $[(^t\text{BuNH})\text{Te}(\mu\text{-N}^t\text{Bu})_2\text{Te}$-

(35) van Bolhjuis, F.; Koster, P. B.; Migchelsen, T. *Acta Crystallogr.* **1967**, *23*, 90.

(36) The strength of the E−I1 (E = N, S, Se) interaction has been estimated in terms of the Pauling relationship between the distance R and the bond order N;[37] $N = 10^{(D - R)/0.71}$, where R is the observed bond length (Å) and D is the single bond length that is estimated by the sums of appropriate covalent radii (Å):[30] N−I, 2.03; S−I, 2.37; Se−I, 2.50 Å.

(37) Pauling, L., *The Nature of the Chemical Bond*, 3rd ed.; Cornell University Press: Ithaca, NY, 1960.

(38) Compound **3** exhibits the strongest N−I1 interaction, resulting in a very long I1−I2 distance that is close to that expected for the ionic interaction. The I2−I3 and I3−I4 bond lengths can be compared to those in I_3^- (see Figure 5).

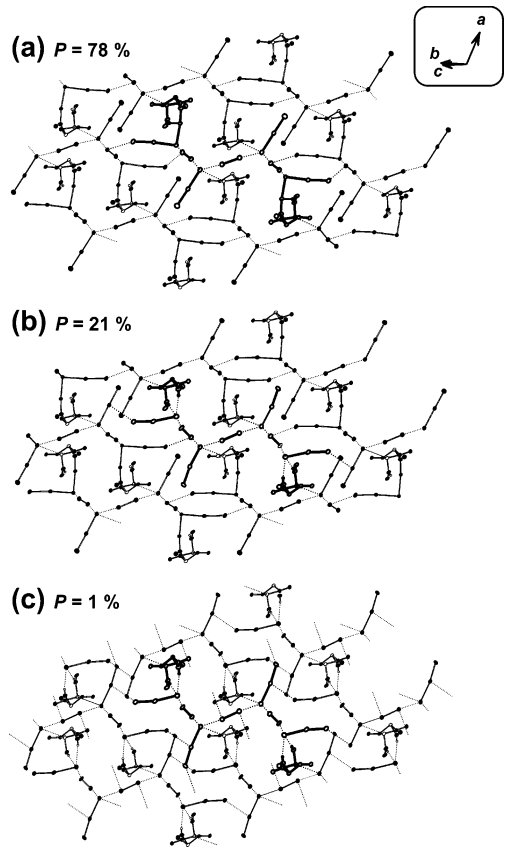

Figure 6. Packing alternatives in the disordered lattice containing **5a**·2MeCN and **5b**·2MeCN. (a) The I···I and Te···I close contacts (<4.0 Å) between the $[(^t\text{BuNH})\text{Te}(\mu\text{-N}^t\text{Bu})_2\text{Te}\{\text{N}(\text{I}_2)_2{}^t\text{Bu}\}]_2(\text{I}_3)_2(\text{I}_2)_3$·2MeCN units (probability of occurrence, 78%). (b) The I···I and Te···I close contacts (<4.0 Å) between the $[(^t\text{BuNH})\text{Te}(\mu\text{-N}^t\text{Bu})_2\text{Te}\{\text{N}(\text{I}_2)_2{}^t\text{Bu}\}]_2(\text{I}_3)_2(\text{I}_2)_3$·2MeCN and $[(^t\text{BuNH})\text{Te}(\mu\text{-N}^t\text{Bu})_2\text{Te}(\text{NH}^t\text{Bu})]_2(\text{I}_3)_4(\text{I}_2)_3$·2MeCN units (probability of occurrence, 21%). (c) The I···I and Te···I close contacts (<4.0 Å) between the $[(^t\text{BuNH})\text{Te}(\mu\text{-N}^t\text{Bu})_2\text{Te}(\text{NH}^t\text{Bu})]_2(\text{I}_3)_4(\text{I}_2)_3$·2MeCN units (probability of occurrence, 1%). The methyl groups of the ^{t}Bu units and the solvent molecules have been omitted for clarity.

$\{\text{N}(\text{I}_2)_2{}^t\text{Bu}\}]_2(\text{I}_3)_2(\text{I}_2)_3$ unit and one $[(^t\text{BuNH})\text{Te}(\mu\text{-N}^t\text{Bu})_2\text{Te}(\text{NH}^t\text{Bu})]_2(\text{I}_3)_4(\text{I}_2)_3$ unit sharing adjacent positions is 21%, and the probability for two **5b** units sharing adjacent positions is 1%. It can be seen from Figure 6 that, although the secondary I···I and Te···I contacts (<4 Å) in different packing alternatives vary slightly, $[(^t\text{BuNH})\text{Te}(\mu\text{-N}^t\text{Bu})_2\text{Te}\{\text{N}(\text{I}_2)_2{}^t\text{Bu}\}]_2(\text{I}_3)_2(\text{I}_2)_3$ and $[(^t\text{BuNH})\text{Te}(\mu\text{-N}^t\text{Bu})_2\text{Te}(\text{NH}^t\text{Bu})]_2(\text{I}_3)_4(\text{I}_2)_3$ can easily substitute one another in the lattice.

NMR and Vibrational Spectra of 5. The ^{1}H NMR spectrum of the red product from the reaction of **4a** with LiI and I_2 (molar ratio 1:1:4.5) in CH_2Cl_2 shows four resonances at 9.04, 1.65, 1.52, and 1.26 ppm in an intensity ratio of 1:18:9:9. The resonance at 9.04 ppm is assigned to the N−H proton. On the basis of the relative intensities, the resonance at 1.65 ppm is assigned to the protons of endocyclic N^{t}Bu groups and the latter two resonances are attributed to the protons of exocyclic N^{t}Bu groups. Consistently, the ^{13}C NMR spectrum shows three resonances at 35.7, 32.9, and 29.3 ppm in an intensity ratio of 2:1:1 that are attributed to the methyl carbon resonances of the N^{t}Bu groups. The presence of the $[(^t\text{BuNH})\text{Te}(\mu\text{-N}^t\text{Bu})_2\text{Te}(\text{NH}^t\text{Bu})]^{2+}$ cation at this stage is not indicated by the NMR spectra. It is probably a hydrolysis product that is formed during the slow recrystallization process as a result of the presence of adventitious water.

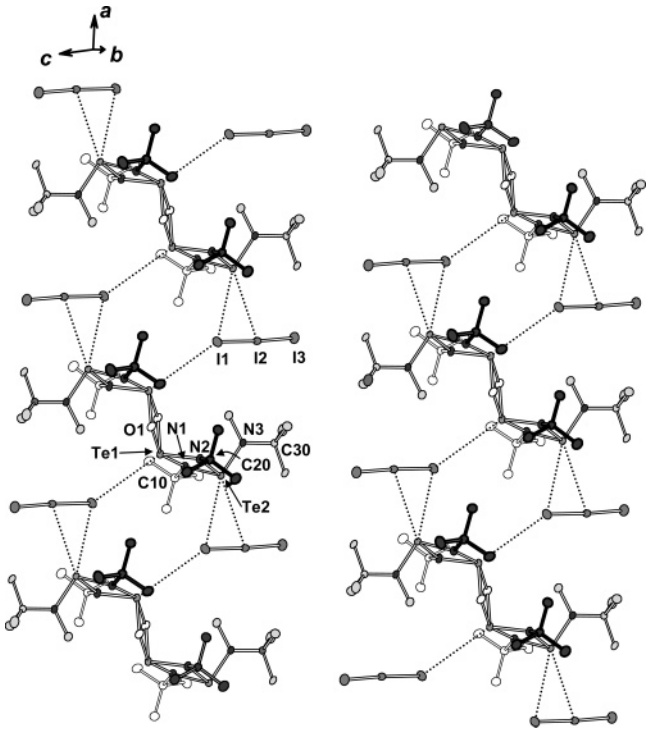

Figure 7. Crystal structure of **6** with the atomic numbering scheme. Thermal ellipsoids are drawn at the 50% probability level. The hydrogen atoms are omitted for clarity.

The IR spectrum of **5** exhibits a weak absorption band at 3275 cm^{-1} assigned to the N−H vibration. The Raman spectrum shows five vibrations at 92(w, sh), 118(w, sh), 140(m, sh), 168(s, sh), and 181(vs) cm^{-1} that are very similar to those reported at 101(m, br), 144(s), 162(s), and 179(m) cm^{-1} for the $I_{18}{}^{4-}$ anion.[39] On the basis of the recent assignments of the Raman spectra of $I_{18}{}^{4-}$ and $I_{16}{}^{4-}$,[39,40] the presence of I_2 and $I_3{}^-$ in the powder of **5** can be inferred. Some of the weak Raman lines at 750−1050 cm^{-1} are probably due to the N−I stretching vibrations.

Formation and Crystal Structure of 6. Reactions of the mono- and dimethylated derivatives of **1**, $[(^t\text{BuNMe})\text{Te}(\mu\text{-N}^t\text{Bu})_2\text{TeN}^t\text{Bu}][\text{OSO}_2\text{CF}_3]$ and $[(^t\text{BuNMe})\text{Te}(\mu\text{-N}^t\text{Bu})_2\text{Te}(\text{MeN}^t\text{Bu})][\text{OSO}_2\text{CF}_3]_2$, respectively, with a mixture of LiI and I_2 in acetonitrile produced moisture-sensitive, dark red powders that contained $\text{Li}[\text{CF}_3\text{SO}_3]$. The NMR spectra of the product of the former reaction exhibited significant shifts in the N−Me resonance compared to those of $[(^t\text{BuNMe})\text{Te}(\mu\text{-N}^t\text{Bu})_2\text{TeN}^t\text{Bu}][\text{OSO}_2\text{CF}_3]$ (2.33−3.25 ppm in the ^{1}H NMR spectrum and 28.4−31.8 ppm in the ^{13}C NMR spectrum).[41] These large shifts suggest a conversion of the monocation $[(^t\text{BuMeN})\text{Te}(\mu\text{-N}^t\text{Bu})_2\text{Te}(\text{N}^t\text{Bu})]^+$ to the dication $[(^t\text{BuMeN})\text{Te}(\mu\text{-N}^t\text{Bu})_2\text{Te}(\text{NI}^t\text{Bu})]^{2+}$, involving the formation of an N−I bond. By contrast, the product of the reaction involving the dimethylated derivative $[(^t\text{BuNMe})$-

(39) Bigoli, F.; Deplano, P.; Devillanova, F. A.; Lippolis, V.; Mercuri, M. L.; Pellinghelli, M. A.; Trogu, M. F. *Inorg. Chim. Acta* **1998**, *276*, 115.
(40) Deplano, P.; Devillanova, F. A.; Ferraro, J. R.; Mercuri, M. R.; Lippolis, V.; Trogu, E. F. *Appl. Spectrosc.* **1994**, *48*, 1236.

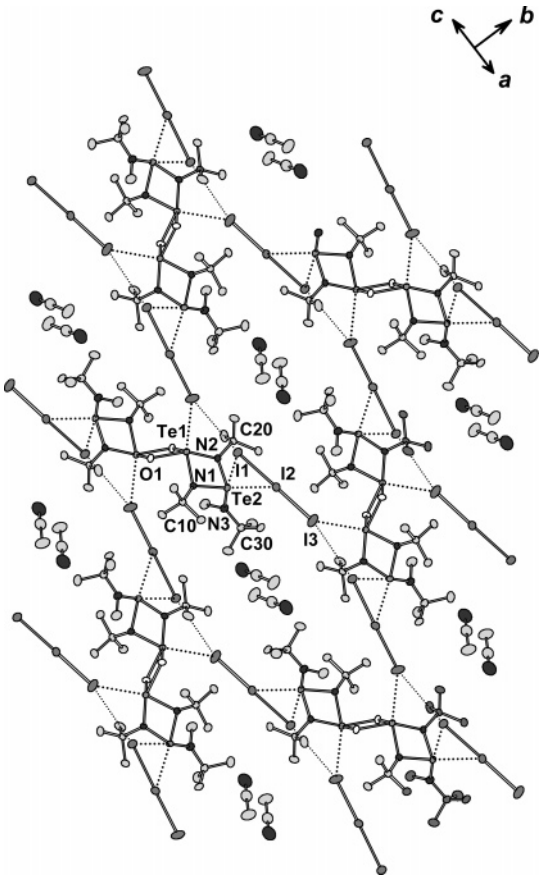

Figure 8. Crystal structure of **6**·2MeCN, indicating the atomic numbering scheme and the Te···I and I···I close contacts. Thermal ellispoids are drawn at the 50% probability level. The hydrogen atoms are omitted for clarity.

Te(μ-N^{t}Bu)$_2$Te(MeN^{t}Bu)][OSO$_2$CF$_3$]$_2$ shows only minor shifts in the N−Me resonances in both the ^{1}H and ^{13}C NMR spectra.[41] In this case, N−I bond formation is preempted, because both terminal N^{t}Bu groups are methylated.

Recrystallization of these products from acetonitrile produced red crystals that were shown by X-ray crystallography to contain the partial hydrolysis product **6**, which was obtained as an acetonitrile solvate **6**·2MeCN in the reaction involving [(^{t}BuNMe)Te(μ-N^{t}Bu)$_2$TeN^{t}Bu][OSO$_2$CF$_3$]. The crystal structures of **6** and **6**·2MeCN, and the atomic numbering scheme, are shown in Figures 7 and 8. The structural parameters are summarized in Table 2. Similarly to the imidotelluroxane dication in **3**, the [(^{t}BuMeN)Te(μ-N^{t}Bu)$_2$] units of the [(^{t}BuMeN)Te(μ-N^{t}Bu)$_2$Te(μ-O)]$_2^{2+}$ dication in **6** and **6**·2MeCN show trans geometry with respect to the central Te$_2$O$_2$ ring (Figures 7 and 8). Although the incorporation of solvent molecules has no significant effect on the bond lengths of the [(^{t}BuMeN)Te(μ-N^{t}Bu)$_2$Te(μ-O)]$_2^{2+}$ dication, an inspection of the bond angles reveals a more open structure in **6**·2MeCN than in **6**. The N3−Te2−Te1 angle increases from 107.5(1)° to 113.78(9)°, and the Te1−Te1−Te2 angle increases from 121.87(3)° to 126.52(1)°.

More significantly, the presence of the MeCN molecules leads to differences in the anion−cation interactions between **6** and **6**·2MeCN, as depicted in Figures 7 and 8, respectively. Whereas the I_3^- anion in **6** exhibits two Te···I close contacts to one dication [Te2···I1 = 3.747(1) Å and Te2···I2 = 3.842(1) Å] and one weak Te···I close contact to another dication [Te1···I1 = 4.015(1) Å], that in **6**·2MeCN shows three Te···I close contacts to one dication [Te2···I1 = 3.7057(9) Å, Te2···I2 = 3.8836(7) Å, and a weak contact Te1···I1 = 4.0089(7) Å]. The Te···I secondary interaction between I_3^- and another dication is significantly stronger than in the case of **6** [Te1−I3 = 3.8647(7) Å]. In addition, **6**·2MeCN exhibits one weak I···I close contact [I1−I3 = 4.039(1) Å] that is less than the sum of the van der Waals radii for two iodine atoms (4.3 Å).[30] This leads to unbranched polyiodide chains of I_3^- units in the lattice of **6**·2MeCN that are absent in the crystal structure of **6**.

We note that the bond parameters of the [(^{t}BuMeN)Te(μ-N^{t}Bu)$_2$Te(μ-O)]$_2^{2+}$ dication in **6** or **6**·2MeCN are rather similar to those of the [(^{t}BuIN)Te(μ-N^{t}Bu)$_2$Te(μ-O)]$_2^{2+}$ dication in **3**. The conformation of the dication in **3** is closer to that in **6**·2MeCN, as indicated by the ∠N3−Te2−Te1 angles [113.2(7), 107.5(1), and 113.78(9)° for **3**, **6**, and **6**·2MeCN, respectively] and by the ∠Te1−Te1−Te2 angles [125.83(9), 121.87(3), and 126.52(1)° for **3**, **6**, and **6**·2MeCN, respectively]. All other metrical parameters of the three cations agree within experimental error.

Acknowledgment. Financial support from the Academy of Finland, Emil Aaltonen Foundation, Finnish Cultural Foundation, and NSERC (Canada) is gratefully acknowledged.

Supporting Information Available: X-ray crystallographic files in CIF format. This material is available free of charge via the Internet at http://pubs.acs.org.

IC050058K

(41) (a) NMR data for [(^{t}BuNMe)Te(μ-N^{t}Bu)$_2$TeN^{t}Bu][OSO$_2$CF$_3$]. ^{1}H NMR (CD$_3$CN): δ 2.33 (3H, N*Me*), 1.46 [9H, C(C*H*$_3$)$_3$, exocyclic N^{t}Bu group], 1.44 [9H, C(C*H*$_3$)$_3$, exocyclic N^{t}Bu group], 1.43 [18H, C(C*H*$_3$)$_3$, endocyclic N^{t}Bu groups]. ^{13}C {^{1}H} NMR (CD$_3$CN): δ 36.94 [3C, C(*C*H$_3$)$_3$, exocyclic N^{t}Bu group], 35.81 [6C, C(*C*H$_3$)$_3$, endocyclic N^{t}Bu groups], 30.95 [3C, C(*C*H$_3$)$_3$, exocyclic N^{t}Bu group], 28.37 (1C, N*Me*). (b) NMR data for [(^{t}BuNMe)Te(μ-N^{t}Bu)$_2$Te(MeN^{t}Bu)][OSO$_2$CF$_3$]$_2$. ^{1}H NMR (CD$_3$CN): δ 3.45 (6H, N*Me*), 1.58 [18H, C(C*H*$_3$)$_3$], 1.54 [18H, C(C*H*$_3$)$_3$]. ^{13}C {^{1}H} NMR (CD$_3$CN): δ 34.17 [6C, C(*C*H$_3$)$_3$], 32.74 (2C, N*Me*), 30.41 [6C, C(*C*H$_3$)$_3$].